Çukurova Üniversitesi Mühendislik Fakültesi Dergisi, 37(1), ss. 93-107, Mart 2022
Cukurova University Journal of the Faculty of Engineering, 37(1), pp. 93-107, March 2022

Flow Characteristics and Heat Transfer Enhancement of Sinusoidal Corrugated Channels with Different Configurations

Veli ÖZBOLAT[*1] ORCID *0000-0002-1757-3054*
Beşir ŞAHİN[2] ORCID *0000-0003-0671-0890*

[1]*Cukurova University, Ceyhan Engineering Faculty, Mechanical Engineering Department, Adana*
[2]*Cukurova University, Engineering Faculty, Mechanical Engineering Department, Adana*

Geliş tarihi: 03.01.2022 Kabul tarihi: 21.03.2022

Atıf şekli/ How to cite: ÖZBOLAT, V., ŞAHİN, B., (2022). Flow Characteristics and Heat Transfer Enhancement of Sinusoidal Corrugated Channels with Different Configurations. Çukurova Üniversitesi, Mühendislik Fakültesi Dergisi, 37(1), 93-107.

Abstract

This study investigated flow characteristics and heat transfer enhancement in various sinusoidal corrugated channels. The channel height and the phase shift effects on the flow structures and thermal performances were examined numerically for Reynolds numbers in the range of 2500≤Re≤7500. The geometrical configurations of this study cover three different channel heights (H_{min}/H_{max}=0.36, 0.54, 0.72) and three phase shift angles (φ=0°, 90°, 180°). Velocity distribution, turbulence intensity, local and averaged Nusselt numbers, and friction factor were calculated for various configurations. Finally, thermal performance factors (TPF) were also calculated to determine the optimum channel configuration and operating condition.

Keywords: Corrugated channel, Heat transfer enhancement, Phase shift, Thermal performance factor

Sinüs Şeklinde Oluklu Kanalların Farklı Konfigürasyonlardaki Akış Karakteristiği ve Isı Transfer İyileştirmesi

Öz

Bu çalışma sinüs şeklindeki çeşitli kanallardaki akış karekteristiğini ve ısı transfer iyileştirmesini incelemiştir. Kanal yüksekliği ve faz açısının akış yapısı ve ısıl performansa etkileri Reynolds sayısı 2500≤Re≤7500 aralığında sayısal olarak incelenmiştir. Bu çalışmadaki geometrik konfigurasyonlar üç kanal boyu (H_{min}/H_{maks}=0,36, 0,54, 0,72) ve üç faz açısını (φ=0°, 90°, 180°) kapsamaktadır. Hız dağılımı, türbülans şiddeti, yerel ve ortalama Nusselt sayıları ve sürtünme faktörü çeşitli konfigürasyonlar için hesaplanmıştır. Son olarak, optimal kanal konfigürasyonu ve çalışma koşulunu belirlemek için ısıl performans faktörü (TPF) de hesaplanmıştır.

Anahtar Kelimeler: Oluklu kanal, Isı transfer iyileşmesi, Faz açısı, Isıl perfomans faktörü

[*]Corresponding author (Sorumlu yazar): Veli ÖZBOLAT, *vozbolat@cu.edu.tr*

1. INTRODUCTION

Heat transfer enhancement in channels is an important topic due to its usage in numerous engineering applications such as heat exchangers, electronic cooling devices, solar collectors, air conditioning systems, etc. Using corrugated walls instead of plain plates is one of the effective methods for improving the thermal performance of channels. Moreover, attaching inserts [1,2], adding nanoparticles to working fluid [3-7], and producing pulsating flow [8-12] can also be applied for extra improvement. Heat transfer enhancement in channels with different corrugation geometries such as sinusoidal [13-17], rectangular [18-20], arc-shaped [21,22], and trapezoidal [23,24] were both studied experimentally and numerically.

Heat transfer enhancement of corrugated channels improves by creating a new boundary layer with a higher temperature gradient on the surface by replacing core fluid [25-27]. Therefore, wavy walls are very effective on heat transfer augmentation in an unsteady flow since they improve interactions between core fluid and boundary layer. On the other hand, the heat transfer rate in corrugated channels does not increase substantially if the flow is steady [17,28]. In addition, the thermal boundary layer breaks and destabilizes by the effect of wavy walls, which work as turbulence promotors to improve local heat and mass transfer [29]. External power input is not needed in this method, but additional power requirements are supplied from the power available in the system which may cause a fluid pressure drop. So using optimum surface design with meaningful pressure loss is an effective way to enhance heat transfer.

Goldstein and Sparrow [30] were probably the first who studied the local heat and mass transfers in wavy wall channels. They studied corrugated wall effects under laminar, transitional, and low Reynolds number turbulent flow regimes. Their results indicated that heat transfer rates increase three folds compared to straight channels in a low Reynolds number turbulent flow regime. However, their effect on improvement has moderate when the flow is laminar. Another study performed by the same group [31] investigated forced convection heat transfer coefficients and friction factors for flow in a corrugated duct for Reynolds number ranging from 1500 to 25000. Their results indicated that heat transfer improved about a factor of 2.5 compared to the parallel plate channel. In addition, they found the magnitude of friction factors, averaging 0.57 which is significantly greater than that of a straight duct. Oyakawa et al. [32] investigated the effects of channel width on heat transfer and flow characteristics of 0° sinusoidal wave channel. They found that pitch (P) to width (H) ratio P/H=2 is optimal for heat transfer augmentation. Oviedo-Tolentino et al. [26] studied chaotic flow mixing control in 180° sinusoidal wavy channel by applying different convergence and divergence angles (0.5°, 1°, and 1.5°) in Reynolds number ranging from 200 to 1200 and compared their results with the sinusoidal wavy channel. The results indicated that diverging channels improve chaotic mixing in channel flows since the flow is more unstable. On the contrary, the flow is very stable even at a high Reynolds number in converging channels. Ramgadia and Saha [33] investigated the thermal performance for different H_{min}/H_{max} ratios (0.1 to 0.5) at Reynolds number range 0-600. They found that H_{min}/H_{max}=0.2 has the highest Termal Performance Factor (TPF) and for all channel heights TPF increases with Reynolds number in unsteady flow while decreases in a steady flow. In addition, heat transfer in sinusoidally wavy channels is higher than parallel plate channels. Hossain and Islam [34] studied the effect of variations of minimum height, amplitude, and wavelength of the sine-shaped wavy channel on heat transfer rate. Their results showed that heat transfer and friction factor increases with increasing amplitude and decreasing channel height since the flow become more unstable. However, they found wavelength variations have limited effect. In a recent study performed by Kurtulmus et al. [14], heat transfer and flow characteristics in a 180° sinusoidal corrugated channel were investigated for Reynolds numbers ranging from 4000 to 10000. They varied the

channel height (H_{min}/H_{max}=0.5, 0.35, and 0.28) and calculated the thermal performance factor (TPF). The results showed that TPF is maximum at Re=4000 for all channel height and the maximum TPF value was obtained as 1.46 for H_{min}/H_{max}=0.5. There are much more studies related to passive methods for improving the thermal performance of corrugated channels than mentioned above. However, they mostly investigated heat transfer augmentation using nanofluids, attaching inserts, varying geometrical parameters. In this study, flow characteristics and thermal performance of sinusoidal corrugated channel for different phase shifts and channel height while keeping sinusoidal wavy wall geometry same.

2. MATERIALS AND METHODS

2.1. Definition of Physical Domain

Heat transfer and flow characteristics of a thirteen wavy section sinusoidal channel have been investigated. The adiabatic smooth sections were added to the inlet and the outlet of the geometry to obtain appropriate boundary conditions, and the flow was considered fully developed at the inlet of the channel [35]. The wavy sections of the geometry consist of two isothermally heated sinusoidal wavy walls with a constant wavelength of (L_w) and amplitude of (a) as seen in Figure 1.

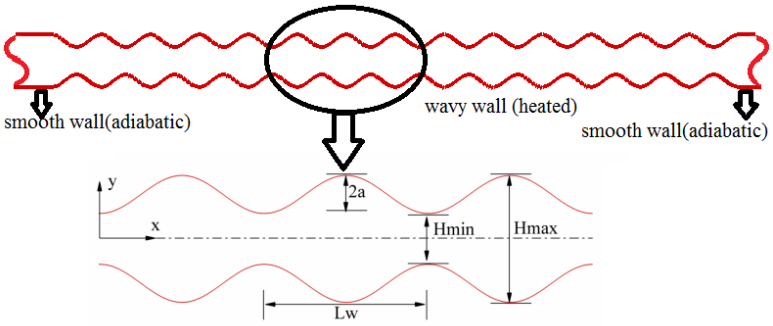

Figure 1. Schematic representation of the 180° phase shift model

The wavy surface function was defined as follow:

$$y=\frac{H_{min}}{2}+a\sin\frac{2\pi x}{L_w} \quad (1)$$

The wavelength and wave amplitude of the wavy walls are 28 mm and 3.5 mm, respectively. With moving the upper wall in x and y directions while keeping the lower wall fixed, phase shift angle (φ=180°, 90°, and 0°) and channel height (H_{min}/H_{max}=0.72, 0.54 and 0.36) were varied, respectively.

2.2. Numerical Computation

The numerical simulations were performed by using fluid simulation software ANSYS Fluent 14.5 (Canonsburg, PA). The governing equations of flow have been discretized by a finite volume method and the pressure-velocity coupling system has been resolved by using the SIMPLE algorithm. The main governing equations are as follows:

Continuity Equation:

$$\frac{\partial u}{\partial x}+\frac{\partial v}{\partial y}=0 \quad (2)$$

Momentum Equation:

$$\frac{\partial u}{\partial t}+u\frac{\partial u}{\partial x}+v\frac{\partial u}{\partial y}=-\frac{1}{\rho}\frac{\partial p}{\partial x}+\upsilon\frac{\partial^2 u}{\partial x^2}+\upsilon\frac{\partial^2 u}{\partial y^2} \quad (3)$$

$$\frac{\partial v}{\partial t}+u\frac{\partial v}{\partial x}+v\frac{\partial v}{\partial y}=-\frac{1}{\rho}\frac{\partial p}{\partial y}+\upsilon\frac{\partial^2 v}{\partial x^2}+\upsilon\frac{\partial^2 v}{\partial y^2} \quad (4)$$

Energy Equation:

$$\frac{\partial T}{\partial t}+u\frac{\partial T}{\partial x}+v\frac{\partial T}{\partial y}=\alpha\left(\frac{\partial^2 T}{\partial x^2}+\frac{\partial^2 T}{\partial y^2}\right) \quad (5)$$

Where

$$\alpha=\frac{\kappa}{\rho.C_p} \quad (6)$$

The k-ε turbulence model introduced by Launder and Spalding [36] is used to solve the numerical problem due to its robustness, economy, and acceptable accuracy for turbulent flow and heat transfer simulations. The turbulent kinetic energy (k) and the rate of turbulent kinetic energy dissipation (ε) are defined, respectively, as:

$$\frac{\partial}{\partial t}(\rho k)+\frac{\partial}{\partial x_i}(\rho k u_i)=\frac{\partial}{\partial x_j}\left[\left(\mu+\frac{\mu_t}{\sigma_k}\right)\frac{\partial k}{\partial x_j}\right]+G_k-\rho\varepsilon \quad (7)$$

$$\frac{\partial}{\partial t}(\rho\varepsilon)+\frac{\partial}{\partial x_i}(\rho\varepsilon u_i)=\frac{\partial}{\partial x_j}\left[\left(\mu+\frac{\mu_t}{\sigma_\varepsilon}\right)\frac{\partial \varepsilon}{\partial x_j}\right]+C_{\varepsilon 1}\frac{\varepsilon}{k}G_k-C_{\varepsilon 2}\rho\frac{\varepsilon^2}{k} \quad (8)$$

Where the rate of turbulent kinetic energy generation is:

$$G_k=-\rho\overline{u_i' u_j'}\frac{\partial u_j}{\partial x_i} \quad (9)$$

The turbulent viscosity, μ_t is calculated by combining k and ε as follows:

$$\mu_t=\rho C_\mu\frac{k^2}{\varepsilon} \quad (10)$$

The following constants can be obtained by comprehensive data fitting for a wide range of turbulent flow [36]:

$C_{\varepsilon 1}=1.4$, $C_{\varepsilon 2}=1.92$, $C_\mu=0.09$, $\sigma_k=1.0$ and $\sigma_\varepsilon=1.3$

Boundary conditions:

A no-slip boundary condition is imposed at the walls, where both velocity components are set to zero. Flat walls at the inlet and outlet of the channel are considered thermally isolated, and a constant wavy walls temperature is set higher than a uniform temperature of the input fluid. To reduce the computational time, a fully developed velocity profile is assigned at the inlet and the flat walls are shortened. The flow is assumed to be two-dimensional, incompressible, and turbulent. In addition, the fluid is Newtonian.

For inlet flow,

$$u_{in}=6\bar{u}\left[0.25-\left(\frac{y}{H}\right)^2\right] \text{ and } T=T_{in} \quad (11)$$

On the walls of the channel:

$u=v=0$ and $T=T_w$ at sinusoidal wavy walls

$T=T_{in}$ at smooth walls

On the axis of the channel:

$$\frac{\partial \bar{u}}{\partial y}=\frac{\partial \bar{v}}{\partial y}=\frac{\partial \bar{T}}{\partial y} \quad (12)$$

To represent the results and characterize fluid flow and heat transfer in a wavy channel, the following parameters are presented.

Reynolds number, Re is defined as:

$$Re=\frac{\rho.\bar{u}.D_h}{\mu} \quad (13)$$

Heat transfer coefficient, h along the wavy surface can be calculated using the following equation:

$$h(x)=\frac{q''(x)}{T_w-T_m} \quad (14)$$

Where T_m is the bulk temperature which can be determined as:

$$T_m=\frac{\int_0^{H/2} u.T.dA}{\int_0^{H/2} u.dA} \quad (15)$$

The local Nusselt number, Nu is defined as:

$$Nu_x=\frac{h_x.D_h}{\kappa} \quad (16)$$

The average Nusselt number, $\overline{Nu}$ along the corrugated wavy wall is calculated by integrating the local Nusselt number, Nu over the wavy section. Therefore, the average Nusselt number is defined as:

$$\overline{Nu}=\frac{1}{L}\int_0^L Nu.dx \quad (17)$$

The friction factor, f for the flow in the corrugated channel is computed as:

$$f=\Delta p\frac{2D_h}{\Delta x(\rho\bar{u}^2)} \quad (18)$$

Using a corrugated wall instead of a smooth one enhances heat transfer inherently comes with additional pressure loss caused by higher friction at the walls due to the flow separation. The thermal performance factor (TPF), as functions of Nusselt number and friction factor, is used to analyze the overall performance since most of the time heat transfer and friction factor increase simultaneously. TPF is defined as:

$$TPF=\frac{\overline{Nu}/\overline{Nu_o}}{\left(f/f_o\right)^{1/3}} \quad (19)$$

Where $\overline{Nu_o}$ and f_o are average Nusselt number and friction factor, respectively for fully developed flow in a flat channel subject to a constant wall temperature.

2.3. Grid Testing and Code Validation

In the present numerical investigation, non-staggered grids which are finer near the boundaries while coarser at the core region (seen in Figure 2) are used since higher gradients of variable values are expected near the walls. The numerical computation is ended if the sum of the absolute residual satisfies the convergence criterion of 10^{-6} for all parameters in the computational domain. A constant time step of 0.001 was used for all calculations.

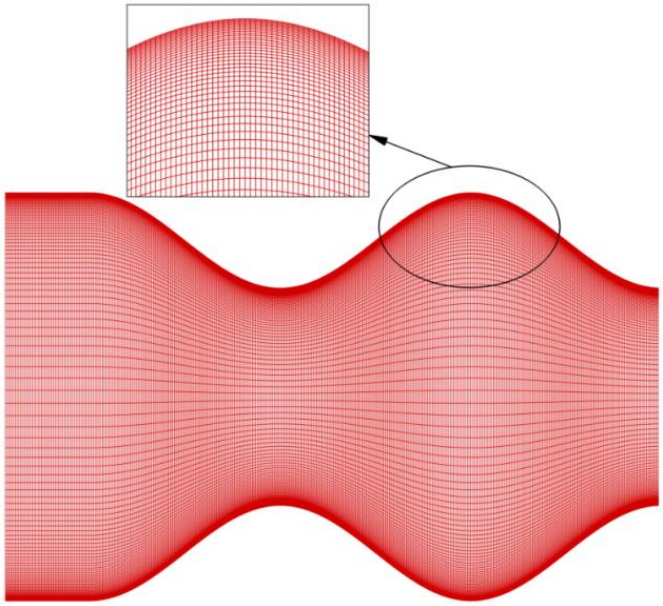

Figure 2. Schematic illustration of a non-uniform and non-orthogonal grid in the computational domain

The accuracy of results depends on the grid resolution. To ensure the accuracy of the numerical computation, the sufficiency of the grid domain for a channel with a phase shift of 180° and H_{min}/H_{max} ratio of 0.54 was tested. Three different mesh combinations (139×65, 160×80, 228×115) for one wave were used to test the number of elements required. Figure 3 shows the axial velocity profiles at the middle of the third wave for Re=2500. Since the deviation between the medium-coarse and fine grid is very small, the results of the fine grid (228×115) are presented in this study.

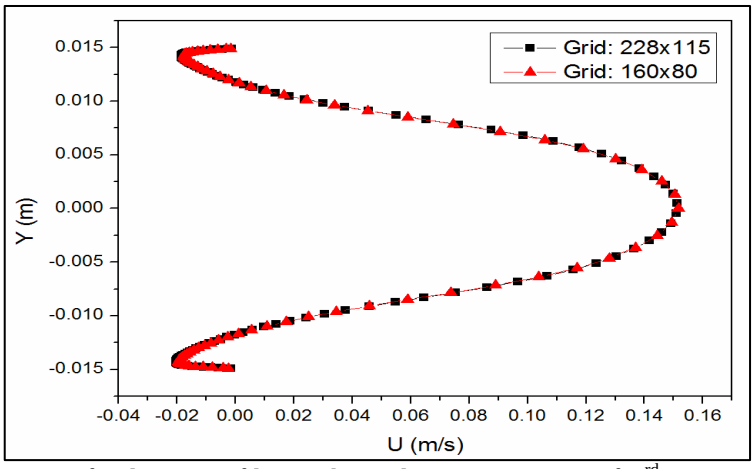

Figure 3. Comparison of velocity profiles at the widest cross-section of 3rd wave of 180° channel at Re=2500 for grids 228x115 and 160x80

3. RESULTS AND DISCUSSIONS

Effects of the channel height and phase shift on heat transfer enhancement of sinusoidal corrugated channels are discussed for three Reynolds numbers. The optimum geometrical configuration and operating condition of the corrugated channel are determined by considering the thermal performance factor (TPF).

Hydrodynamics of water flow in corrugated channels with three channels heights H_1 (H_{min}/H_{max}=0.36), H_2 (H_{min}/H_{max}=0.54), and H_3 (H_{min}/H_{max}=0.72) are studied and the obtained results are compared with each other and that of the parallel plate channels to demonstrate the channel height effects on the thermal-hydraulic characteristics. The numerical simulations have been done for Reynolds numbers of 2500, 5000, and 7500.

Figure 4a presents streamwise velocity, u distributions along the axis in the corrugated channels with 180° phase shift angle for H_1, H_2, and H_3. It is seen in this Figure that the maximum velocity is observed for H_1 since the distance between the upper and the lower walls is the shortest. Distributions of streamwise velocity component illustrate that streamwise velocity profiles along the axis of the channels are periodic. H_1 has the highest amplitude of the periodic velocity distributions among all cases. However, streamwise velocity for H_3 seems almost straight line along the channel axis since the amplitude of sinusoidal wavy walls are very small concerning channel height. It can also be said that the periodicity of streamwise velocities eventually becomes stable in the region downstream of second cavities. Moreover, the streamwise velocity decreases in diverging sections and increases in converging sections of the wavy channel. The amplitude of streamwise velocity variation on the axis also depends on the Reynolds number. As can be seen from Figure 4b, the amplitude of the streamwise velocity on the axis is small for low Reynolds number such as Re=2500 and become bigger as the Reynolds number increases.

Using sinusoidal corrugated walls instead of parallel plates leads to magnifying turbulence intensity through the corrugated channel. The rate of turbulence intensity varies with a channel height. As can be seen from Figure 4c, the rate of turbulence intensity through the corrugated channel increases with decreasing the distance between the upper and the lower walls. Increasing the flow mixing and turbulence intensity improves the thermal transport through the corrugated channel with pressure drop penalty. Hence, additional considerations are required to find optimum design parameters.

Figure 4d illustrates the pressure distribution along the axis in the wavy part of the sinusoidal corrugated channel with a configuration of channel height H_2 (H_{min}/H_{max}=0.54) and phase shift angle, φ =180° at the Reynolds number of 2500. As the flow moves towards the converging section of the channel, pressure decreases rapidly in the flow direction since the core flow region becomes narrow. On the other hand, rapid axial static pressure increase occurs as the fluid moves from the converging section to the diverging section due to the expansion of the core flow after the narrowest cross-section. The periodic variations in axial static pressure occur throughout the sinusoidal corrugated channel since the channel geometry changes periodically too. Therefore, axial static pressure distribution along the wave repeats identical variation through the other waves. Moreover, the rate of pressure variations depends on the wave parameters (amplitude and wavelength), the channel height, and the Reynolds number.

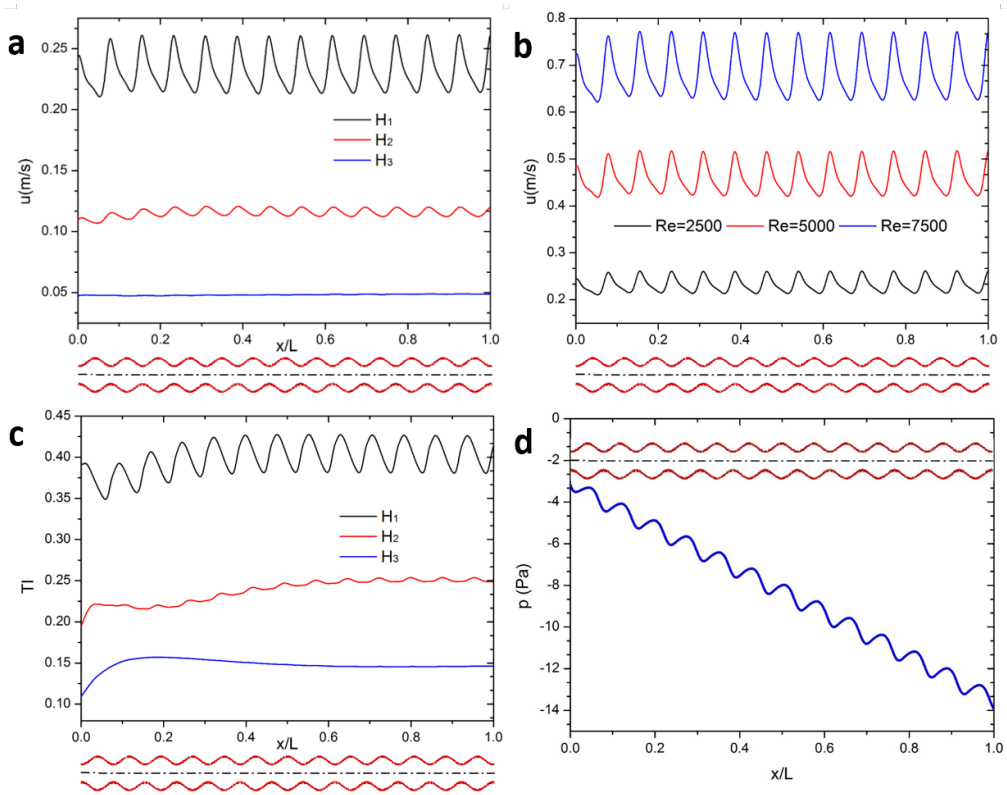

Figure 4. a) Distributions of streamwise velocities along the channel axis with 180° phase angle for Re=2500, b) Distributions of streamwise velocities along the axis of channel H_1 with 180° phase angle, c) Distributions of turbulence intensities along the channel axis with 180° phase angle for Re=2500, d) Axial statistic pressure distribution along the channel axis with 180° phase angle for Re=2500

The distance between the upper and the lower walls of a corrugated channel is an important parameter that influences the heat transfer performance and frictions. The influence of the corrugated channel height on the averaged Nusselt number for 0° phase shift angles is illustrated in Figure 5a. For certain phase shift angles, the averaged Nusselt number is seen to increase significantly with increasing the Reynolds number. It is also shown that the averaged Nusselt number

obtained in the case of the highest channel height (H_3) is lower than that from the lower ones (H_1 and H_2) for a given phase shift angle due to the lower velocities. Reduction in the wall velocity gradients cause an increase in the thermal boundary layer. The maximum heat transfer occurs in the case of H_1 (H_{min}/H_{max}=0.36) at Reynolds number of 7500. As can be seen in Figure 5a, H_1 has the maximum increment rate of averaged Nusselt number, $\overline{Nu}$ with Reynolds number for 0° phase shift angle. Recirculation develops in the corrugation troughs as the fluid flows through the corrugated surface, and improves the mixing of fluid in the boundary layer so the heat transfer in a corrugated channel enhances.

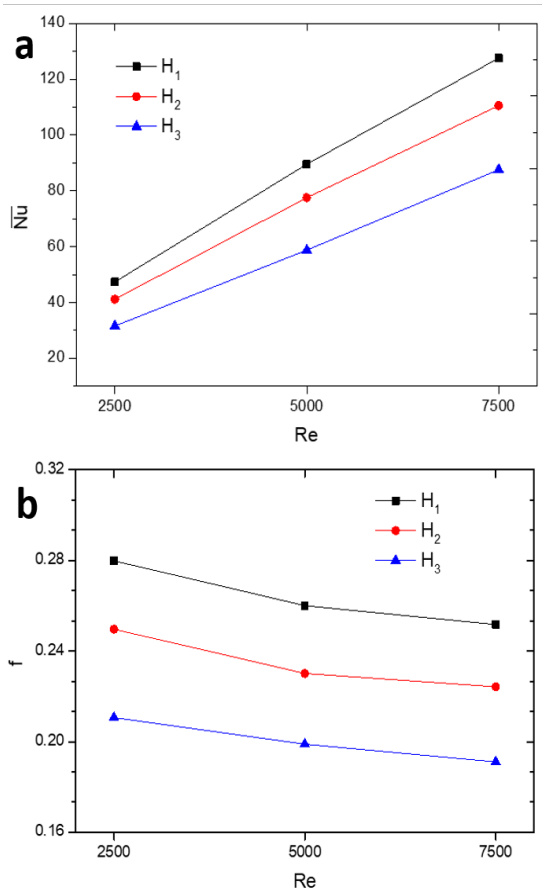

Figure 5. Variations of a) the averaged Nusselt number and b) the friction factor with Reynolds number for the corrugated channels with phase angle, φ=0°

The friction factor, f is a main hydraulic characteristic of flow and is influenced by the development of turbulence in corrugated channels. Therefore it is mainly affected by Reynolds number and channel configurations concerning channel height and phase shift angle. Friction factor as a function of Reynolds number for flow in 0° phase shift angle corrugated channel at different channel heights (H_{min}/H_{max}=0.36, 0.54, and 0.72) are plotted in Figure 5b. This Figure shows that the friction factor gradually decreases with increasing Reynolds numbers for any value of the channel height. In addition, the friction factor gets higher values as the channel becomes narrower. The friction factors for all corrugated channel configurations have much higher than that for the straight channel since corrugations promote unstable formed vortices in the core of the corrugated channel's flow, causing a significant increase of pressure drops. It can be seen that the channel height, H_{min}/H_{max}=0.36 has the highest friction factor. On the other hand, the lowest values of friction factors are observed at H_{min}/H_{max}=0.72 for all Reynolds numbers considered.

Figure 6 shows the effects of the phase shift angle, φ on the streamwise velocities, u and turbulence intensities, TI from the wavy part of the channel H_1. As shown in Figure 6(a-c), using wavy plates develops harmonic velocity distributions on the axis of the channel. For all the phase shift angles, the wavelengths and amplitudes of the velocity become stable after certain distances. The distance obtained for the same wavelength and amplitude is shortest for the 180° phase shift angle since the upper and the lower walls are symmetrical from the beginning of the channel. It is also noted that the amplitude of the velocity distribution depends on the phase shift angle and Reynolds number. The amplitude of the velocity distribution increases with the phase shift angle and Reynolds number. The highest amplitude is observed for the channel with a 180° phase shift angle at Re=7500. Corrugated plates lead to turbulence along the axis of the channel. In Figure 6(d-f), the strong dependence of the turbulence intensity on the phase shift angle and Reynolds number is also noticed. For all the geometric configurations tested, the turbulence intensity rate increases with Reynolds number.

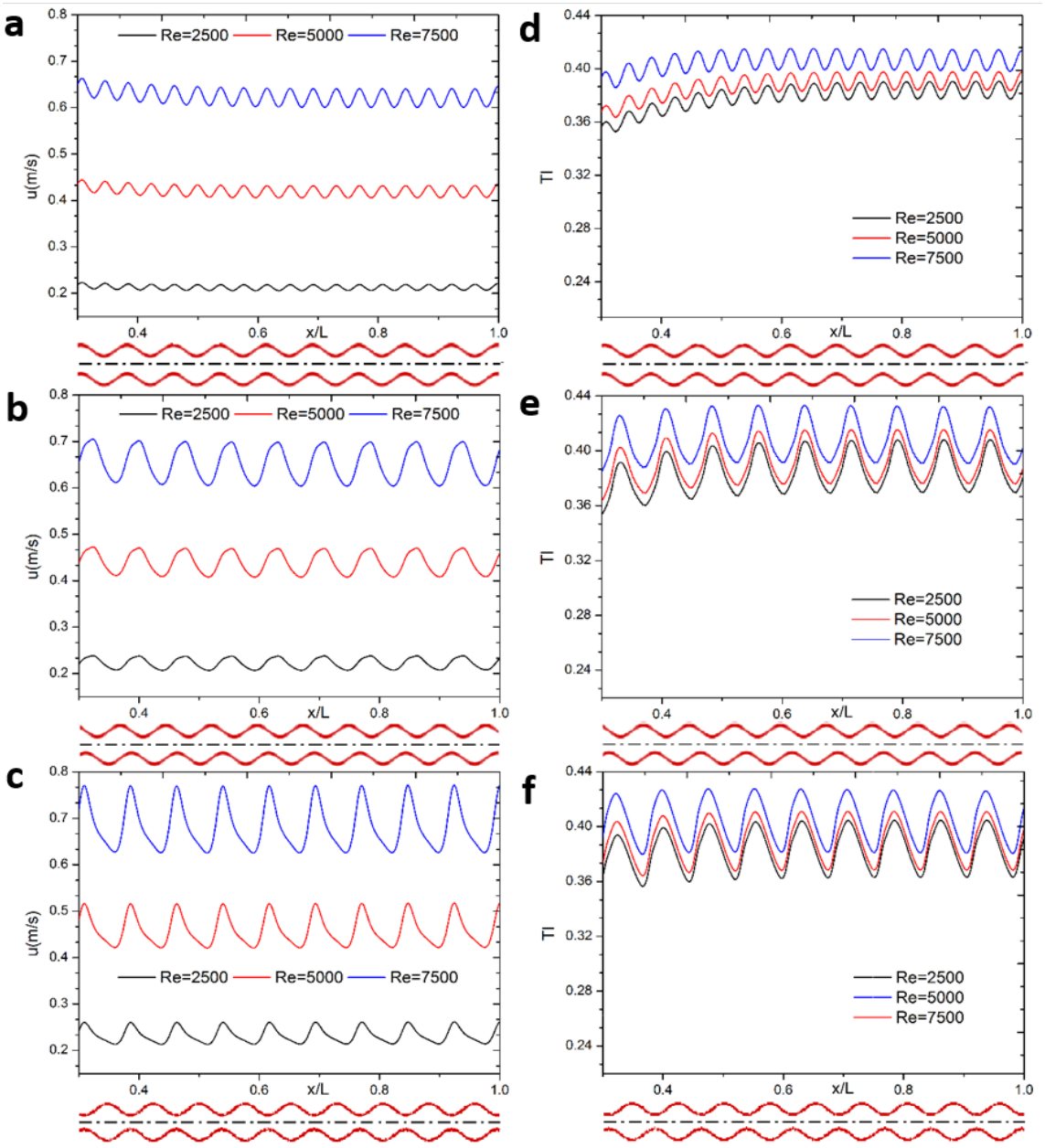

Figure 6. Distributions of streamwise velocities for phase shift angles, φ of a) 0°, b) 90° and c) 180°, and turbulence intensities along the channel axis for phase shift angles, φ of d) 0°, e) 90° and f) 180°

Figure 7 shows Nusselt number values along the straight channel for Reynolds numbers of 2500, 5000, and 7500. Nusselt number is maximum at the inlet and decreases slightly since the boundary layer is thinnest at the inlet of the channel and its thickness increases with axial distance along the channel wall.

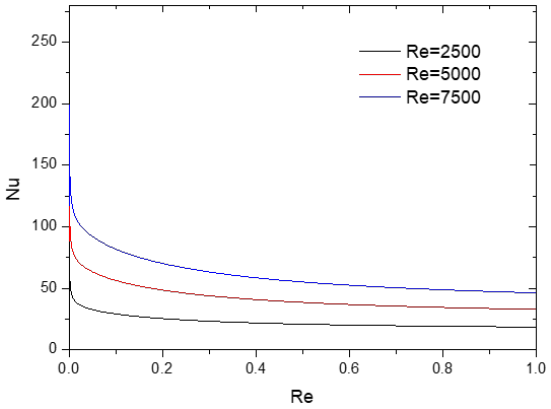

Figure 7. Variations of the local Nusselt numbers, along the lower wall of the straight channel

The variations of the local Nusselt number with Reynolds number along the lower wavy walls of the corrugated channels with phase shift angles of 0°, 90°, and 180° are shown in Figure 8. The local Nusselt number in the converging section of each wave is higher than that in the diverging section since the channel becomes narrower over the throats resulting in a higher velocity gradient in the converging section, which increases the heat transfer ratio. Therefore, the peaks of the local Nusselt number are observed at the channel throats due to the sudden increase in velocity gradient. In addition, the local Nusselt number increases with the Reynolds number for all the phase shift angles. Although the local Nusselt number values change with Reynolds number, similar trends are observed for certain phase shift angles. Moreover, the Nusselt number of corrugated channels for all phase shift angles is higher than that of the straight channel at all the Reynolds numbers.

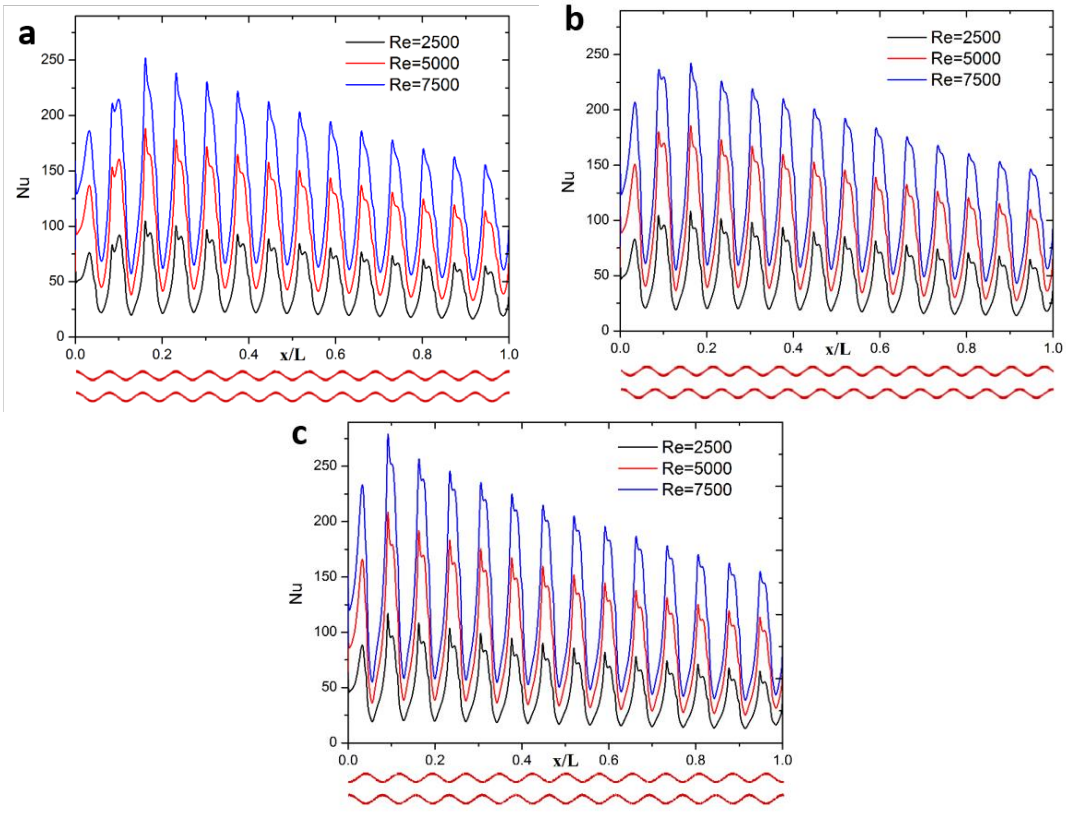

Figure 8. Variations of the local Nusselt numbers along the lower wavy walls for different phase shift angles, φ of the channel H_1 a) 0°, b) 90° and c) 180°

The averaged Nusselt numbers, $\overline{Nu}$ as a function of Reynolds number for both corrugated channels (φ=0°, 90°, 180°) and straight channel are presented in Figure 9a. Increasing Reynolds number increases the temperature gradients in the boundary layer region near walls, enhancing the average Nusselt number and the heat transfer from the wall. In addition, heat transfer enhancement due to using corrugated plates at a high Reynolds number is higher compared to the case of a low Reynolds number since the mixing of fluid in the corrugated channel improves with increasing Reynolds number. Also, decreasing the phase shift angle causes a larger re-circulation region and higher swirl flows intensity in the corrugation trough which improves the averaged Nusselt number. Moreover, the averaged Nusselt number values of corrugated channels for all the phase shift angle configurations have a higher value than that of the straight channel case. It can be seen in Figure 9a, the channel with a 0° phase shift angle has the highest averaged Nusselt number at all the Reynolds numbers considered in this study.

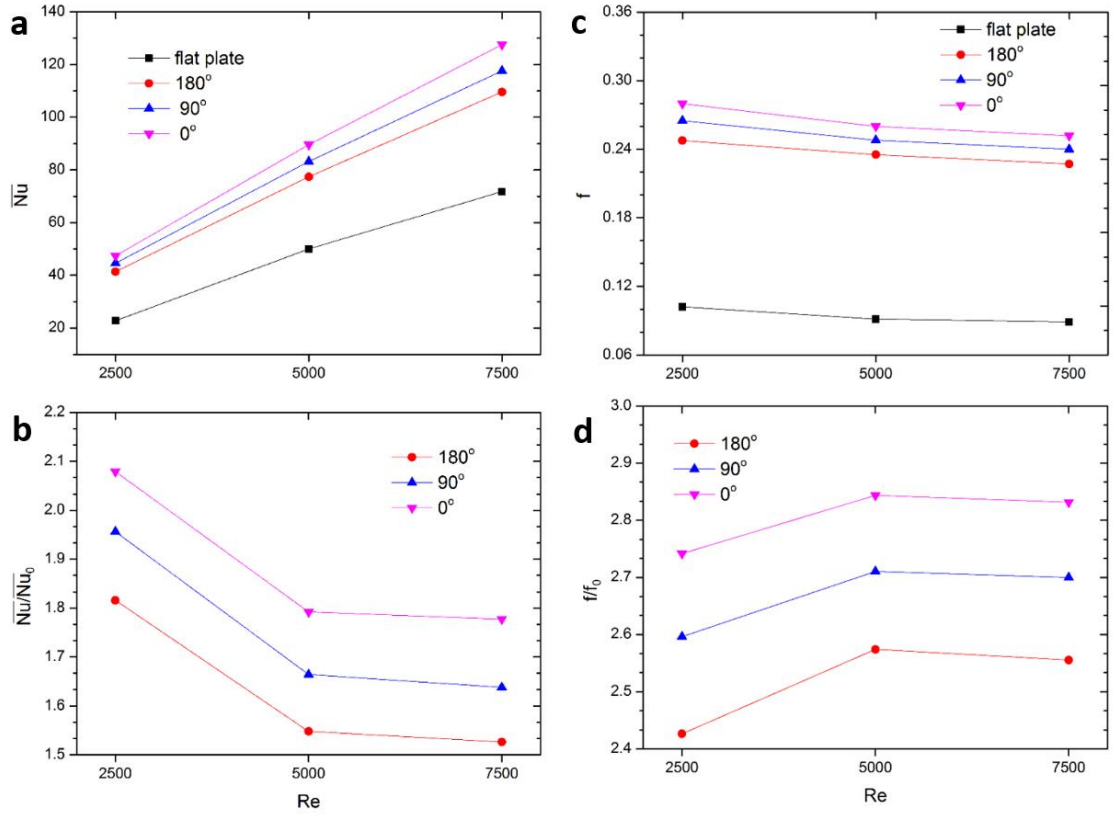

Figure 9. a) Variations of the averaged Nusselt numbers with Reynolds number for corrugated channels (H_1) and the flat plate, b) comparison of the averaged Nusselt numbers of corrugated channels with that of the flat plate, c) variations of the friction factors with Reynolds number for corrugated channels (H_1) and the flat plate, d) comparison of the friction factors of corrugated channels with that of the flat plate

The averaged Nusselt number in the corrugated channels enhances several folds, depending upon the values of Reynolds number and phase shift angle for a given channel height. The heat transfer

rates in corrugated channels of 0°, 90°, and 180° phase shift angles are increased by a factor of 1.78, 1.64, and 1.53 compared to those of straight channel, respectively at the Reynolds number of 7500. On the other hand, the heat transfer enhancement rates increase up to 2.08, 1.96, and 1.82 for 0°, 90°, and 180° phase shift angles, respectively, at Re=2500 (Figure 9b).

Thermal transport is improved by increasing the rate of flow mixing which results in more pressure drops. The measured pressure drops among the simulated corrugated channels are used to predict the friction factors. The friction factor variations with Reynolds numbers for straight channel and corrugated channels (H_{min}/H_{max}=0.36) at different phase shift angles are shown in Figure 9c. The friction factor investigated through wavy channels is larger than that of the straight channel due to the suppression of the viscous sub-layer. In addition, the friction factor decreases with the increase of phase shift angle. It can be observed from Figure 9c that the friction factor decreases with increasing Reynolds numbers for straight channel and all the configurations of corrugated channels. For straight channel, an increase in Reynolds number results in decreasing the laminar sub-layer thickness which reduces the friction factor. Using corrugations causes to block fluid flow and increase the pressure drop, Δp along the channel. Although the pressure drop increases with increasing Reynolds number, the friction factor decreases with an increase in Reynolds number since the friction factor depends on $\Delta p/(\rho u^2)$ and it is inversely proportional with the square of the velocity. The friction factor values for phase shift angle of 0° is the highest among all configurations for all considered Reynolds numbers while the lowest values are observed for a phase shift angle of 180°. The lowest friction factor enhancement is observed at Reynolds number of 2500 for all the phase shifts. The friction factors in corrugated channels with 0°, 90° and 180° phase shift angles increase by a factor of 2.74, 2.59, and 2.43 compared to those of straight channel, respectively at Reynolds number of 2500 (Figure9d).

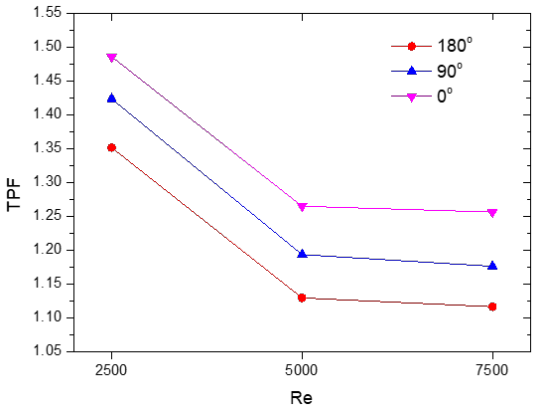

Figure 10. Variations of the thermal performance factors (TPF) with Reynolds number for a corrugated channel (H_1) with phase shifts 0°, 90° and 180°

Heat transfer enhancement in corrugated channels comes with additional frictional losses since corrugated channel disturbs the entire flow field. Therefore, it is necessary to evaluate the net enhancement obtained from using such channels. In this study, the relative thermal-hydraulic performance enhancement is evaluated by the thermal performance factor (TPF) expressed from equation 19.

The variations of the thermal performance factor (TPF) with the phase shift and Reynolds number are presented in Figure 10. A high value of TPF indicates good thermal-hydraulic performance. This Figure shows that TPF decreases with increasing Reynolds number. For the tested three regimes of Reynolds number (Re=2500, 5000, and 7500), TPF decreases with increasing the phase shift angle. The highest TPF is observed for flow in a corrugated channel with a phase shift angle of 0°. The maximum TPF at the Reynolds number of 2500 for the phase shift angles 0°, 90°, and 180° are calculated as 1.48, 1.42, and 1.35, respectively. The channel of φ=0° gives the best TPF at a low Reynolds number regime (Re=2500). Moreover, using corrugated channels at lower Reynolds numbers seems to be more efficient than at higher Reynolds numbers.

4. CONCLUSION

In the present study, numerical simulations have been performed to investigate the thermal-hydraulic characteristics of water flow in sinusoidal corrugated channels. The averaged Nusselt number, the friction factor, and the thermal performance factor (TPF) were calculated for different channel heights (H_{min}/H_{max}=0.36, 0.54, 0.72), phase shift angles (φ=180°, 90°, 0°) over three flow regions (Re=2500, 5000, and 7500). In steady flow, the large recirculation vortices in the upper and the lower waves isolated warmer fluid, which restrains mixing of the warmer fluid with cool fluid passing through the center of the channel. Therefore, the heat transfer does not enhance considerably in steady flow cases. As the Reynold number increases, the recirculation magnitude gets smaller and fresh fluid into the core region moves close to the wave furrows so that heat transfer enhances. Since the core flow is forced to follow the waves of the surrounding geometry in the channel with a phase shift angle of 0°, a higher rate of interactions occurs with recirculation. Hence, φ=0° is the case where significant mixing appears first among all shift angles investigated in this study. The main findings are summarized as follows; (i) Using a corrugated channel enhances heat transfer with an increase in friction factor. The average Nusselt number of sinusoidal corrugated channels enhances up to 2.08 folds, and the friction factor increases up to 2.74 times compared to the parallel plate channel depending on Reynolds number, phase shift angle, and height of the corrugated channel. (ii) The friction factor and Nusselt number increase with decreasing the phase shift angles and increasing Reynolds number for any channel heights considered. (iii) Among all configurations over the tested range of Reynolds numbers, the channel with H_{min}/H_{max}=0.36 and φ=0° at Reynolds number=2500 has the highest TPF.

5. REFERENCES

1. Akbarzadeh, M., Maghrebi, M.J., 2018. Combined Effects of Corrugated Walls and Porous Inserts on Performance Improvement in a Heat Exchanger Channel. International Journal of Thermal Science, 127, 266–276.

2. Akbarzadeh, M., Rashidi, S., Karimi, N., Omar, N., 2019. First and Second Laws of Thermodynamics Analysis of Nanofluid Flow Inside a Heat Exchanger Duct with Wavy Walls and a Porous Insert. Journal of Thermal Analysis and Calorimetry, 135, 177-194.

3. Ahmed, M.A., Shuaib, N.H., Yusoff, M.Z. Al-Falahi, A.H., 2011. Numerical Investigations of Flow and Heat Transfer Enhancement in a Corrugated Channel Using Nanofluid. International Communications in Heat and Mass Transfer, 38, 1368–1375.

4. Ahmed, M.A., Shuaib, N.H., Yusoff, M.Z., 2012. Numerical Investigations on the Heat Transfer Enhancement in a Wavy Channel Using Nanofluid. International Journal of Heat and Mass Transfer, 55, 5891–5898.

5. Ozbolat, V., Sahin, B., 2013. Numerical Investigations of Heat Transfer Enhancement of Water-based Al_2O_3 Nanofluids in a Sinusoidal-wall Channel. Heat Transfer and Thermal Engineering (American Society of Mechanical Engineers) 8A, 1–6.

6. Tokgoz, N., Ozbolat, V., Sahin, B., 2016. Investıgatıon of Heat Transfer Enhancement by Using Al_2O_3/Water Nanofluıd in Rectangular Corrugated Channel. Kahramanmaras Sutcu Imam University Journal of Engineering Sciences, 19, 42–51.

7. Ajeel, R.K., Salim, W.S.-I.W., Hasnan, K., 2019. Thermal Performance Comparison of Various Corrugated Channels Using Nanofluid: Numerical Study. Alexandria Engineering Journal, 58, 75–87.

8. Jafari, M., Farhadi, M., Sedighi, K., 2015. Convection Heat Transfer of SWCNT-Nanofluid in a Corrugated Channel Under Pulsating Velocity Profile. International Communications in Heat and Mass Transfer, 67, 137–146.

9. Kurtulmuş, N., Sahin, B., 2020. Experimental Investigation of Pulsating Flow Structures and Heat Transfer Characteristics in Sinusoidal Channels, International Journal of Mechanical Sciences, 167, 105268.

10. Blythman, R., Persoons, T., Jeffers, N.,

Murray, D.B., 2019. Heat Transfer of Laminar Pulsating Flow in a Rectangular Channel. International Journal of Heat and Mass Transfer**,** 128, 279–289.

11. Jafari, M., Farhadi, M., Sedighi, K., 2013. Pulsating Flow Effects on Convection Heat Transfer in a Corrugated Channel: A LBM approach. International Communications in Heat and Mass Transfer, 45, 146–154.

12. Zhang, F., Bian, Y., Liu, Y., Pan, J., Yang, Y., Arima, H., 2019. Experimental and Numerical Analysis of Heat Transfer Enhancement and Flow Characteristics in Grooved Channel for Pulsatile Flow. International Journal of Heat and Mass Transfer, 141, 1168–1180.

13. Ozbolat, V., Tokgoz, N., Sahin, B., 2013 Flow Characteristics and Heat Transfer Enhancement in 2D Corrugated Channels International Journal of Mechanical, Aerospace, Industrial, Mechatronic and Manufacturing Engineering, **7,** 539–543.

14. Kurtulmuş, N., Zontul, H., Sahin, B., 2020. Heat Transfer and Flow Characteristics in a Sinusoidally Curved Converging-diverging Channel. International Journal of Thermal Sciences, 148, 106163.

15. Rush, T.A., Newell, T.A., Jacobi, A.M., 1999 An Experimental Study of Flow and Heat Transfer in Sinusoidal Wavy Passages. International Journal of Heat and Mass Transfer, 42 1541–1553.

16. Rashidi, S., Akbarzadeh, M., Masoodi, R., Languri, E.M., 2017. Thermal-hydraulic and Entropy Generation Analysis for Turbulent Flow Inside a Corrugated Channel. International Journal of Heat and Mass Transfer, 109, 812–823.

17. Wang, G., Vanka, S., P., 1995. Convective Heat Transfer in Periodic Wavy Passages. International Journal of Heat and Mass Transfer, 38**,** 3219–3230.

18. Tokgoz, N., Sahin, B., 2019. Experimental Studies of Flow Characteristics in Corrugated Ducts. International Communications in Heat and Mass Transfer, 104, 41–50.

19. Tokgoz, N., Tunay, T., Sahin, B., 2018. Effect of Corrugated Channel Phase Shifts on Flow Structures and Heat Transfer Rate. Experimental Thermal and Fluid Science, 99, 374–391.

20. Tokgoz, N., Aksoy, M.M., Sahin, B., 2017. Investigation of Flow Characteristics and Heat Transfer Enhancement of Corrugated Duct Geometries. Applied Thermal Engineering, 118, 518–530.

21. Paisarn, N., 2010. Study on the Heat-transfer Characteristics and Pressure Drop in Channels with Arc-shaped Wavy Plates Journal of Engineering Physics and Thermophysics, 83, 1061–1069.

22. Bahaidarah, H.M.S., 2007. A Numerical Study of Fluid Flow and Heat Transfer Characteristics in Channels with Staggered Wavy Walls. Numerical Heat Transfer; Part A: Applications, 51, 877–898.

23. Bahaidarah, H.M., 2009. Fluid Flow and Heat Transfer Characteristics in Sharp Edge Wavy Channels with Horizontal Pitch. Emirates Journal for Engineering Research, 14, 53–63.

24. Ahmed, M.A., Yusoff, M.Z., Shuaib, N.H., 2013. Effects of Geometrical Parameters on the Flow and Heat Transfer Characteristics in Trapezoidal-corrugated Channel Using Nanofluid. International Communications in Heat and Mass Transfer, 42, 69–74.

25. Oviedo-Tolentino, F., Romero-Méndez, R., Hernández-Guerrero, A., Girón-Palomares, B., 2008. Experimental Study of Fluid Flow in the Entrance of a Sinusoidal Channel International Journal of Heat and Fluid Flow, 29, 1233–1239.

26. Oviedo-Tolentino, F., Romero-Méndez, R., Hernández-Guerrero, A., Girón-Palomares, B., 2009. Use of Diverging or Converging Arrangement of Plates for the Control of Chaotic Mixing in Symmetric Sinusoidal Plate Channels, Experimental Thermal and Fluid Science, 33, 208–214.

27. Tatsuo, N., Shinichiro, M., Shingho, A., Yuji K, 1990. Flow Observations and Mass Transfer Characteristics in Symmetrical Wavy-walled Channels at Moderate Reynolds Numbers for Steady Flow. International Journal of Heat and Mass Transfer, 33, 835–845.

28. Nishimura, T., Ohori, Y., Kawamura, Y., 1984. Flow Characteristics in a Channel with Symmetric Wavy Wall for Steady Flow. Journal of Chemical Engineerıng of Japan, 17,

466–471.

29. Gradeck, M., Hoareau, B., Lebouché, M., 2005. Local Analysis of Heat Transfer Inside Corrugated Channel. International Journal of Heat and Mass Transfer, 48, 1909–1915.

30. Goldstein, L., Sparrow, E., M., 1977. Heat/Mass Transfer Characteristics for Flow in a Corrugated Wall Channel. Journal of Heat Transfer, 99, 187–195.

31. O'Brien, J.E., Sparrow, E.M., 1982. Corrugated-duct Heat Transfer, Pressure Drop and Flow Visualization, Journal of Heat Transfer, 104, 410–416.

32. Oyakawa, K., Shinzato, T., Mabuchi, I., 1989. The Effects of the Channel Width on Heat-transfer Augmentation in a Sinusoidal Wave Channel. JSME International Journal, 32, 403-410.

33. Ramgadia, A.G., Saha, A.K., 2012. Fully Developed Flow and Heat Transfer Characteristics in a Wavy Passage: Effect of Amplitude of Waviness and Reynolds Number International Journal of Heat and Mass Transfer, 55, 2494–2509.

34. Hossain, M.Z., Islam, A.K.M.S., 2004. Fully Developed Flow Structures and Heat Transfer in Sine-shaped Wavy Channels. International Communications in Heat and Mass Transfer, 31, 887–896.

35. Ozbolat, V., 2015. Flow Characteristics and Heat Transfer Enhancement of Sinusoidal Corrugated Channels. PhD Thesis, Cukurova University Institute of Natural and Applied Sciences, 143.

36. Launder, B.E., Spalding, D.B., 1974. The Numerical Computation of Turbulent Flows. Computer Methods in Applied Mechanics and Engineering, 3, 269–289.